Journal of Engineering and Applied Sciences 12 (Special Issue 5): 6884-6891, 2017
ISSN: 1816-949X

Automatic Centroid-Node Adaptive Meshless (CNAM) Method for Solving Convection-Diffusion Problems

[1]Nissaya Chuathonga, [2]Sayan Kaennakham and [1]Wattana Toutip
[1]Department of Mathematics, Faculty of Science, Khon Kaen University,
40002 Khon Kaen, Thailand
[2]School of Mathematics, Institute of Science, Suranaree University of Technology,
30000 Nakhon Ratchasima, Thailand

Abstract: There are two main objectives of this Research. Firstly, it aims to numerically solve problems under convection-diffusion category by RBF-collocation type of meshfree method. Secondly, the research proposes a simple but effective automatic node adaptive algorithm which is constructed and also embedded in the computing process. The two main tasks are combined forming what we name as an automatic 'Centroid-Node Adaptive Meshless (CNAM)' method. All solutions obtained using CNAM are validated again other numerical work, corresponding exacts and also those obtained without CNAM (or with conventional nodes). It has been clearly shown from all examples that CNAM is capable of reproducing some challenging physics phenomenon such as boundary layers with satisfactory level of accuracy.

Key words: Node adaptive, RBF-collocation method, convection-diffusion, work proposes, CNAM, numerically

INTRODUCTION

Convection diffusion problems are governed by typical mathematical models appearing in many branches of sciences and engineering such as biological, physical chemical, physical in fluid mechanics, astrophysics, meteorology and multiphase flow in oil reservoirs, polymer flow and many other areas (Djidjeli *et al*., 2004). Convection diffusion equations consist of two different phenomena, convection and diffusion. Solving these equations is an important and challenging problem. In the study of this type of problem, traditionally the numerical solution in many cases has been tackled using the Finite Difference Method (FDM) the Finite Element Method (FEM), Boundary Element Method (BEM) or the Finite Volume Method (FVM). For FDM, FEM and FVM before the computing process can be performed the mesh generation in a domain is required to take place making the methods rather difficult and time-consuming particularly when dealing with higher dimensional problems with complicated geometry. In the last two decades, some alternative methods that do not require mesh generation have been rapidly obtaining a huge amount of interest. These methods are known as meshless or meshfree methods. The idea and the main advantage of these methods is that they only need a set of scattered point within domain to evaluate the numerical solution. In other words there is no relationship among the scattered points. Several meshless methods have also been reported in the literature for example the domain-based methods including the element-free Galerkin method (Belytschko *et al*., 1994) the local boundary integral equation method (Sladek *et al*., 2000) and the Radial Basis Functions (RBFs) approach (Sarra and Kansa, 2009; Kansa, 1990a, b). In this research, we focus on one called radial basis function collocation proposed by Kansa (1990a, b).

Adaptive techniques are useful tools to enhance the quality of the numerical solutions with a minimal computational effort. Most current adaptive techniques used in conjunction with meshless method, refines the solution either adding new nodes or changing the position of existing nodes such that the computation al error is reduced as much as possible. As meshless method require only a set of arbitrarily distributed nodes without requiring connectivity information, they can easily exploit adaptive techniques because nodes can be easily added and deleted or moved (Lin and Atluri, 2000; Li *et al*., 2003). There are several adaptive methods that have been used in conjunction with the meshless methods. Gomez *et al*. (2006) built a global refinement technique for Kansa's unsymetric collocation approach solving steady state partial differential equations by using the local node refinement technique purposed by Behrens and Iske

Corresponding Author: Sayan Kaennakham, School of Mathematics, Institute of Science, Suranaree University of Technology, 30000 Nakhon Ratchasima, Thailand

(2002), Behrens *et al.* (2001) and a quad-tree type algorithm (Berger and Jameson, 1985; Boztosun and Charafi, 2002). Zhang and Wang (2010) applied a stencil of the finite difference method and build up the new iterative scheme to solve the implicit difference equation for solving the numerical solution of the two dimensional convection diffusion. It is found that the new scheme has the same parallelism and a higher rate of convergence than the Jacobi Iteration. Libre *et al.* (2008) present a wavelet based adaptive scheme and investigated the efficiency of this scheme for solving nearly singular potential PDEs. The wavelet coefficients then were used as an estimation of the sensible regions for node adaption. It has been show that the proposed adaptive scheme can detect the singularities both in the domain and near the boundaries. GU and Liu (2006) proposed several techniques to overcome the instability issues in convection dominated phenomenon including the enlargement of the local support domain the upwind support domain the adaptive upwind support domain the biased support domain the nodal refinement and the adaptive analysis.

MATERIALS AND METHODS

Mathematical background

RBF-collocation method

Definition 2.1: Fasshauer (2007) a function $\Phi: \mathbb{R}^d \to \mathbb{R}$ with dimension d is called radial provided there exists a univariate function $\varphi:[0, \infty) \to \mathbb{R}$ such that $\Phi(x) = \varphi(r)$ where $r = \|x\|$, $x \in \mathbb{R}^d$ and $\|.\|$ is some norm on $\mathbb{R}^d$-usually the Euclidean norm. The methodology starts with considering a linear elliptic partial differential equation with boundary conditions where g(x) and f(x) are known. We seek $\mu(x)$ from:

$$L(x)=f(x),\ x \text{ in } \Omega \tag{1}$$

$$M(x)=g(x),\ x \text{ on } \partial\Omega \tag{2}$$

Where:

$\Omega \subset \mathbb{R}^d$, $\partial\Omega$ = Denotes the boundary of domain Ω

L and M = The linear elliptic partial differential operators and operating on the domain Ω and boundary domain $\partial\Omega$, respectively

For Kansa's method it represents the approximate solution $\tilde{u}(x)$ by the interpolation, using an RBF interpolation as the following:

$$\tilde{u}(x)=\sum_{J=1}^{N} c_j \varphi(\| x - x_j \|) \tag{3}$$

We can see that N linear dependent equations are required for solving N unknowns of c_j. Substituting $\tilde{u}(x)$ into Eq. 1 and 2 we obtain the system of equations as follows:

$$\sum_{j=1}^{N} c_j L\varphi(\|x - x_j\|) = f(x_i), x_i \in I, i=1, ..., N_1 \tag{4}$$

$$\sum_{j=1}^{N} c_j M\varphi(\|x - x_j\|) = g(x_i), x_i \in B, i = N_1+1, ..., N \tag{5}$$

Where:

N = Collocation points on both domain Ω and boundary domain $\partial\Omega$ and divide it into N_1 Interior points

N_B = Boundary points ($N = N_1+N_B$)

$X = \{x_1, \ldots, x_N\}$ = The set of collocation points

$I = \{x_1, \ldots, x_{N1}\}$ = The set of interior points

$B = \{x_{N1+1}, \ldots, x_N\}$ = The set of boundary points

The centers x_j used in Eq. 4 and 5 are chosen as collocation points. The previous substituting yields a system of linear algebraic equations which can be solved for seeking coefficient c by rewriting Eq. 4 and 5 in matrix form as:

$$Ac=F \tag{6}$$

Where $c = (c_1, \ldots, c_N)^T$ is the coefficient vector, $F = (f(x_1), ..., f(x_{N1}), g(x_{N1+1}), ..., g(x_N))^T$, $A = (A_L, A_M)^T$ is the N×N matrix, $(A_L)_{ij} = L\varphi(\|x_i - x_j\|)$, $i = 1, ..., N_1$, $j = 1, ..., N$ and $(A_M)_{ij} = M\varphi(\|x_i - x_j\|)$, $i = N_1+1, ..., N$, $j = 1, ..., N$. The unknowns 'c' can be obtained by solving Eq. 6. Therefore, the approximated solution of problems as expressed in at any points in Eq. 1 and 2 the domain can be obtained by substituting c_j into Eq. 3.

The Centroid-Node Adaptive Meshless (CNAM) method: When an automatic node adaptive algorithm is performed properly the resulting node distribution is expected to be optimal for the problem at hand because the solution is used to determine where more nodes are needed. Therefore, it is one of the primary goals of using node adaptive methods that we aim to reduce the numerical error in the digital solution with minimal numerical cost. In this study, we proposed a simple but rather effective node adaptive algorithm where the areas of interest where high errors are expected are identified via a simple error indicator defined as follows.

Definition 2.2: Let $u_{i,j}(t)$ be a numerical solution obtained by using the collocation method at time t and at the node in the domain with coordinate (i, j). The error indicator, noted by E_{ij} is defined as:

$$E_{i,j} = (\Delta_{cell})^w \left|\nabla u_{i,j}\right| \tag{7}$$

where $\Delta_{cell} = \Delta x \Delta y$ = the volume weight w = 1, $|.|$ is the Euclidean norm and the gradient ∇.

Definition 2.3: Let N be the number of the uniformly-distributed nodes in the computational domain Ω and $E_{i,j}$ be the error indicator at node (i, j). The normalized error indicator, $e_{i,j}$ is defined as:

$$e_{i,j} = \frac{E_{ij}}{\max\{E_{i,j}\}}, i,j = 1,...,N \quad (8)$$

Definition 2.4: Let N be the number of the uniformly-distributed nodes in the computational domain Ω and $e_{i,j}$ be the normalized error indicator at node (i, j). Then an area of interest is the subset, Ωk⊆Ω, defined by:

$$\Omega_k = (i,j)\left|e_{i,j} \geq \theta_{th}\right. \quad (9)$$

where θ_{th} the threshold provided by the user and the areas of interest are the union of Ω_k, k = 1, ..., N. The solution gradient ∇ is numerically computed using the central-finite difference. The normalization means, Eq. 8 is needed to prevent the algorithm from producing a strong change of the raw values of solution during the computation which would necessitate a readjustment of the refine threshold θ_{th}. The CNAM algorithm is carried out simply by marking the node of interest with a specified value of θ_{th}, based on the normalized error indicator, $e_{i,j}$ that has been obtain using $u_{i,j}(t)$. Then, it refines the node in such a way as described in Fig. 1. The way to insert additional nodes when a refinement process takes place is done using the centroid of a triangle that contains the node of interest itself and the two nearest neighbor nodes before the approximation and collocation process of the meshless method is then repeated to get a new set of solution, $u_{i,j}(t)$ using the solution at the previous time step as the initial condition (i.e, $u_{i,j}(t-\Delta t)$). This is where the name of Centroid-Node Adaptive Meshless (CNAM) comes from.

Computation details

Implementation for convection-diffusion problem: Consider the governing partial differential equation of convection diffusion problems expressed as:

$$\frac{\partial u}{\partial t} - \alpha\left(\frac{\partial^2 u}{\partial x^2} + \frac{\partial^2 u}{\partial y^2}\right) + \beta\left(\frac{\partial u}{\partial x} + \frac{\partial u}{\partial y}\right) = R \quad (10)$$
$$(x,y) \in \Omega \subset \mathbb{R}^d, t>0$$

Where:

α, β = The diffusive term and convective term, respectively

R = Describes source or sinks of the quantity u

In steady state case, the convection-diffusion Eq. 10 is reduced to the following form:

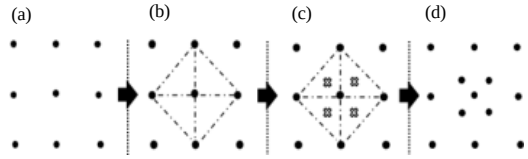

Fig. 1: a-d) Centroid-node adaptive for uniform node distribution; assuming the node in the middle of (a) is marked and subjected to refinement procedure

$$-\alpha\left(\frac{\partial^2 u}{\partial x^2} + \frac{\partial^2 u}{\partial y^2}\right) + \beta\left(\frac{\partial u}{\partial x} + \frac{\partial u}{\partial y}\right) = R(x,y) \in \Omega \subset \mathbb{R}^d \quad (11)$$

In this practice its boundary condition is of dirichlet type as follows:

$$u = 0 \text{ on } \partial\Omega \quad (12)$$

In order to implement the RBF collocation procedure Eq. 1-3, 6 and 11 it is necessary to solve the following linear system:

$$\sum_{j=1}^{N} c_j \left[-\alpha\left(\frac{\partial^2 \varphi\left(\left\|x_i - x_j\right\|\right)}{\partial x^2} + \frac{\partial^2 \varphi\left(\left\|x_i - x_j\right\|\right)}{\partial y^2} \right) + \beta\left(\frac{\partial \varphi\left(\left\|x_i - x_j\right\|\right)}{\partial x} + \frac{\partial \varphi\left(\left\|x_i - x_j\right\|\right)}{\partial y} \right) \right] = R, i = 1,...,N_1 \quad (13)$$

$$\sum_{j=1}^{N} c_j \varphi\left(\left\|x_i - x_j\right\|\right) = 0, i = N_1+1,...,N \quad (14)$$

This system can be written in the form of:

$$\sum_{j=1}^{N} c_j \left[-\alpha[\nabla^2 \varphi] \right]_{ij} + \beta\left[\nabla \varphi\right]_{ij} = R, i = 1,...,N_1 \quad (15)$$

$$\sum_{j=1}^{N} c_j \varphi_{ij} = 0, i = N_1+1,...,N \quad (16)$$

The approximate solutions then can be obtained by substituting the coefficients c_j, obtained by solving the above system in Eq. 3. In time dependent case, Eq. 10 is may be written in the form of:

$$\frac{du}{dt} = Lu \text{ in } \Omega \quad (17)$$

where L is an operator. Equation (17) is discretized in space with meshless method and then it is written in the system of ordinary differential equations as follows:

$$\frac{du}{dt} = F(u) \quad (18)$$

RESULTS AND DISCUSSION

Numerical demonstrations and general discussion: The methodology implemented as detailed in the previous section is now tested out by applying to four examples. The results provided by the method proposed in this research are validated against both the corresponding exacts and those from other numerical studies if available.

Example 1: As the first test case, we consider the Franke-type function (Driscoll and Heryudono, 2007) in $[-1, 1]^2$ which has been used by many authors to test the RBF interpolation:

$$f(x,y) = e^{-0.1}(x^2+y^2)+e^{-0.5}((x-0.5)^2+(y-0.5)^2)e^{-15}((x+0.2)^2+(y+0.4)^2)+e^{-9}((x+0.8)^2+(y-0.8)^2) \quad (19)$$

The CNAM is applied to this function to firstly demonstrate its general figure of performance. The node distribution began with that shown in Fig. 2a and the final node distribution after using CNAM is depicted in Fig. 2b. The solution contours and surface, together also with its corresponding node distribution are shown in Fig. 2c and d, respectively. It is clear that CNAM can perform well for this first test case.

Example 2: In this case, we consider the following potential boundary value problem (Libre *et al*., 2008) in the rectangle domain $\Omega = [0, 1]^2$:

$$\frac{\partial^2 u}{\partial x^2}+\frac{\partial^2 u}{\partial y^2} = f(x,y) \in \Omega \quad (20)$$

The analytical solution is given by:

$$u^{exact} = \tanh(a(y-(v+\mu x))) \quad (21)$$

where a = 15, v = 0.4 and μ = 0.2. Table 1 contains error obtained by CNAM when measured using the same norm of error expressed as:

$$\text{Relative error norm} = \sqrt{\frac{\sum_{i=1}^{N}\left(u_i^{exact}-u_i^{num}\right)^2}{\sum_{i=1}^{N}\left(u_i^{exact}\right)^2}} \quad (22)$$

It is seen that CNAM is capable of numerically reproduce the solutions that are in a very good agreement with the exact. Figure 3 shows the comparison of solution surfaces obtained from using CNAM alongside with it's resultant node distribution (Table 2).

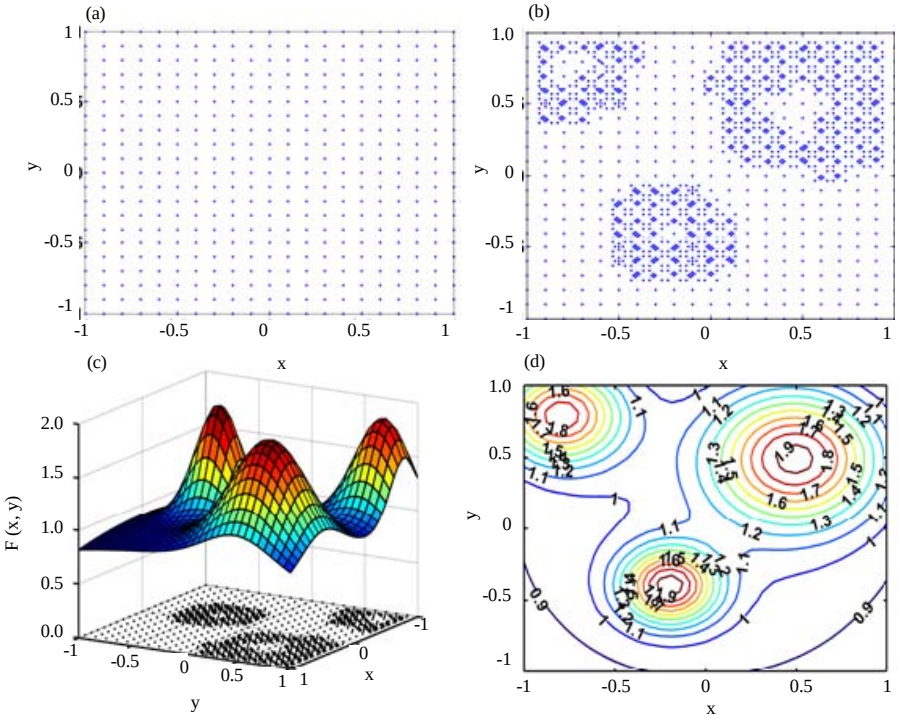

Fig. 2: Overall performance of CNAM for the Franke-type; a) equation with 289 initial nodes and b) 1,117 final nodes

Table 1: Error comparisons between non-adaptive conventional solution and adaptive node solution using CNAM at different numbers of initial nodes and with $\theta_{th} = 0.4$; (RMSE: Root Mean Square Error, MAXE: Maximum Error)

	RMSE		MAXE		Rel.err norm	
No.of initial nodes	Conventional	CNAM	Conventional	CNAM	Conventional	CNAM
25	1.27E-01	8.73E-02	5.95E-01	5.65E-01	1.06E+01	7.24E+00
49	4.64E-02	1.36E-03	2.64E-01	1.11E-02	3.84E+00	1.13E-01
64	1.74E-02	6.43E-04	9.12E-02	4.25E-03	1.44E+00	5.33E-02
81	1.27E-02	2.27E-03	8.78E-02	2.70E-02	1.05E+00	1.88E-01

Table 2: Relative error norm (Rel.err norm)obtained from employing the CNAM algorithm with different MQ shape parameter σand levels of refinement at $\theta_{th} = 0.2$

σ- MQ	Level of refinement	Fnode	Rel.err norm	C-Time (sec)
4.5	2	435	2.7907	1.1377
5.0	2	446	1.2914	1.1227
5.5	2	446	0.7729	1.1638
6.0	2	446	0.4802	1.2060
6.5	2	446	0.3174	1.1947
6.7	2	446	0.2771	1.1220
5.5	3	597	0.9087	2.2365
6.7	3	602	0.2524	2.6741
7.5	3	602	0.1928	2.7373
7.5	4	764	0.2003	4.9538
8.2	4	764	0.1807	5.0613

Here with 169 initial node/conventional nodes which yields the Rel.err norm = 2.8417 and requires 0.0654 s of C-time (Fnode: the number of final nodes, C-Time: computational time)

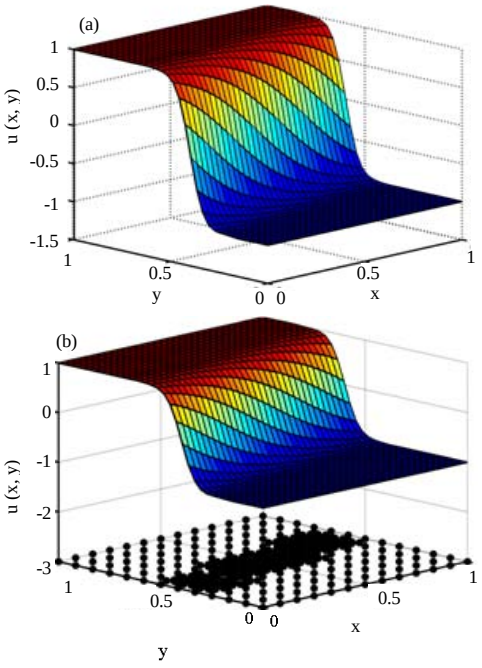

Fig. 3: Solution surface comparison; a) Exact; b) CNAM

Example 3: A benchmark 2D steady state of convection-diffusion problem (Gu and Liu, 2006) is focused on in this example. The governing equation is as follows:

$$L(u) = v^T.\nabla^T(D\nabla u) + \beta u - q(x) = 0 \text{ in } \Omega \qquad (23)$$

The problem domain is $(x, y) \in \Omega = [0, 1]\times[0, 1]$ and the coefficients in Eq. 23 are:

$$D = \begin{bmatrix} \varepsilon & 0 \\ 0 & \varepsilon \end{bmatrix}, v = \{3\text{-}x, 4\text{-}y\} \text{ and } \beta = 1$$

in which ε is a given constant of diffusion coefficient. The boundary condition are considered as $u|_{x=0,\,x=1,\,y=0,\,y=1} = 0$. The exact solutions for this problem is given by:

$$u^{exact} = \sin(x)\left(1\text{-}e^{\frac{2(1-x)}{\varepsilon}}\right)y^2\left(1\text{-}e^{\frac{2(1-y)}{\varepsilon}}\right) \qquad (24)$$

It should be, first of all, stated that this classical example is one of the challenges for any numerical methods proposed in literature. With its boundary layer formation taking place at the domain corner this is well-known to cause instability in solution process. Table 3 provides the relative norm error, Eq. 22 as also used by Gu and Lui (2006) who investigated this problem and concluded that with the diffusive coefficient ε, getting smaller the more difficult it becomes to reproduce the boundary layor with high accuracy. In particular it is clear from Table 3 that when the problem becomes convective-dominated, i.e., $\varepsilon = 0.001$ the relative error can reach up to 195.345 while CNAM can dramatically improve the solutions and noticeably reduce the relative error down to 9.557 which is absolutely remarkable.

In comparison with non-refined conventional node distribution, it can be seen from Table 1 again that without CNAM the error is approximately 100 times higher than that with CNAM.

Figure 4 clearly shows the effectiveness of the CNAM algorithm where the solutions are impressively improved. At different levels of convective force in the system it is shown in Fig. 5 that with smaller ε more nodes are involved in the process as expected. The highest number of nodes generated by CNAM is 1.382 and can produce the solutions with as low as 10.8922 in relative error norm.

Example 4: As the final example, we investigate the problem under the unsteady state (Driscoll and Heryudono, 2007) which the following governing Eq. 25:

Table 3: Error comparisons between non-adaptive solution (Conventional) and adaptive node solution (CNAM) at different numbers epsilon Eq. 23 and with θ_{th} = 0.4 and 441 internal initial/conventional nodes

	Gu and Liu (2006)	Conventional		CNAM		
ε	Rel.err norm	Rel.err norm	Time (sec)	Rel.err norm	Fnode	Time (sec)
100	000.245	00000.0033	0.2240	00.0175	1708	2.6467
10	000.255	00000.0035	0.2108	00.0072	1776	2.0629
1	000.346	00000.0064	0.2112	00.0079	1996	6.0984
0.1	001.276	00000.1980	0.2206	00.5571	600	3.4350
0.01	015.832	00351.9199	0.2424	06.9518	583	0.8907
0.001	195.345	00885.8930	0.2235	09.5576	854	1.3838
0.0001	-	10139.6916	0.2103	10.8922	655	1.2594

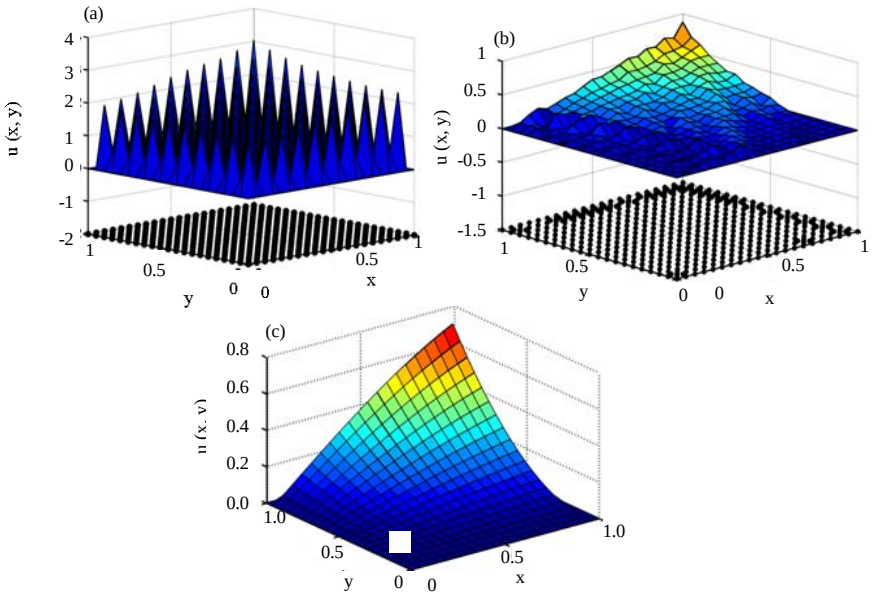

Fig. 4: Surface solution comparisons at ε = 0.0001; a) Conventional without CNAM; b) with CNAM and c) Exact

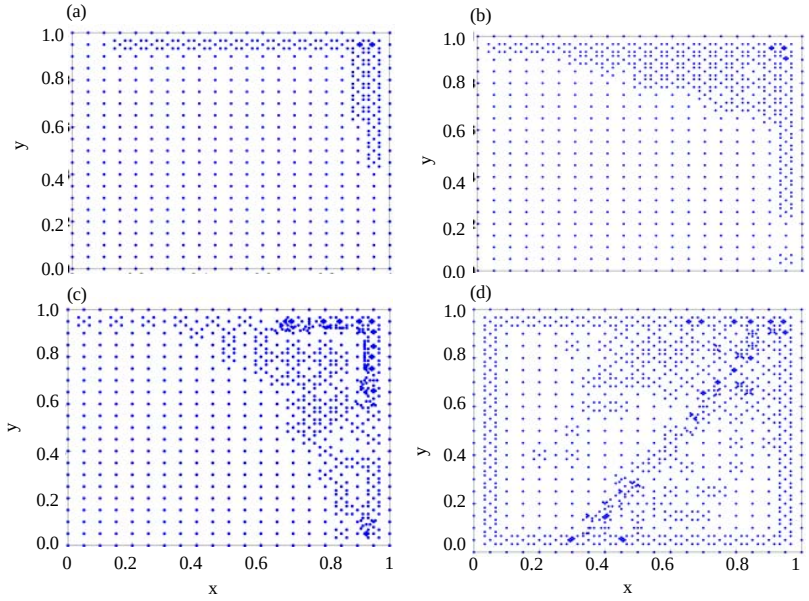

Fig. 5: Node distributions obtained from applying the CNAM; a) ε = 0.1; b) ε = 0.01; c) ε = 0.001 and d) ε = 0.0001

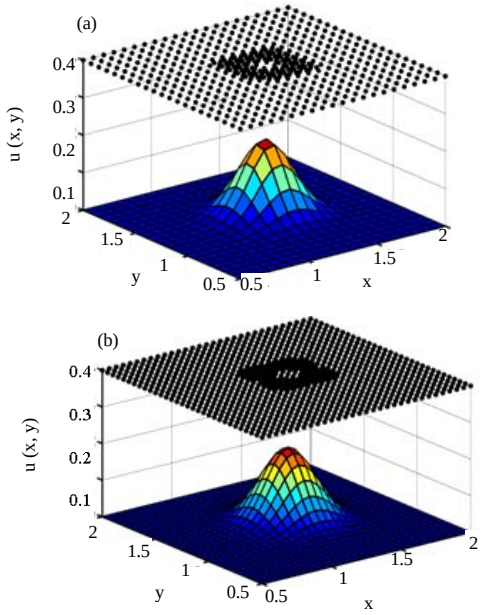

Fig. 6: Solution and its corresponding node distribution when using the CNAM algorithm at time t = 1 sec; a) with 441 initial nodes and b) with 961 initial nodes

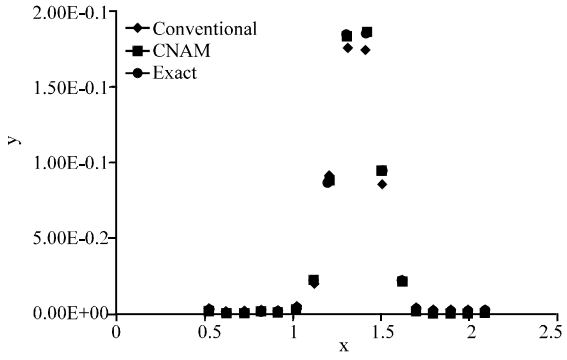

Fig. 7: Comparison of solution on the x = y straight line, obtained from the CNAM algorithm with the vertical axis being the solutions

$$\frac{\partial u}{\partial t}+0.8\left(\frac{\partial u}{\partial x}+\frac{\partial u}{\partial y}\right)=0.01\left(\frac{\partial^2 u}{\partial x^2}+\frac{\partial^2 u}{\partial y^2}\right) \quad (25)$$

Its exact solution is expressed as:

$$u(x,y,t)=\frac{1}{4t+1}\exp\left[-\frac{(x-0.8t-0.5)^2}{0.04(4t+1)}-\frac{(y-0.8t-0.5)^2}{0.01(4t+1)}\right] \quad (26)$$

where (xy)ϵ D = {0.5<x, y<2}, t ϵ (0, T) The initial condition and the boundary condition comes from the exact solution. For time-dependence problems, CNAM is set to perform at the last time step. Figure 6 provides different final node distributions produced at different initial nodes. The solutions obtained from using CNAM are noticeably superior to those with non-refinement/conventional nodes as clearly displayed in Fig. 7.

CONCLUSION

In this study, we propose a new and simple method of node refinement algorithm designed specifically to apply in conjunction with the RBF-collocation meshless method. The idea is based on space-gradient of solution acting as the error indicator where the node of interest is refined following the centroid idea of a triangle. We named this algorithm the Centroid-Node Adaptive Meshless (CNAM) method and demonstrated its capability with some well-known and rather benchmark examples, both steady and time-dependence states. All solutions obtained using CNAM are validated again other numerical work, corresponding exacts and also those obtained without CNAM (or with conventional nodes). It has been clearly shown from all examples that CNAM is capable of reproducing some challenging physics phenomenon such as boundary layers with satisfactory level of accuracy. The limitation of the current version of CNAM is however, to deal with non-uniformly distributed nodes and this is to be our further development.

ACKNOWLEDGEMENT

The first researcher would like to express great appreciation to Science Achievement Scholarship of Thailand (SAST) for their kind financial support.

REFERENCES

Behrens, J. and A. Iske, 2002. Grid-free adaptive semi-Lagrangian advection using radial basis function. Comp. Math. Appl., 43: 319-327.

Behrens, J., A. Iske and S. Pohn, 2001. Effective Node Adaption for Grid-Free Semi-lagrangian Advection. In: Discrete Modeling and Discrete Algorithms in Continuum Mechanics, Sonar, T. and Thoma, I. (Eds.). Logos Verlag Berlin GmbH, Berlin, Germany, pp: 110-119.

Belytschko, T., Y.Y. Lu and L. Gu, 1994. Element-free Galerkin methods. Int. J. Numer. Methods Eng., 37: 229-256.

Berger, M.J. and A. Jameson, 1985. Automatic adaptive grid refinement for the euler equations. AIAA. J., 23: 561-568.

Boztosun, I. and A. Charafi, 2002. An analysis of the linear advection-diffusion equation using mesh-free and mesh-dependent methods. Eng. Anal. Boundary Elem., 26: 889-895.

Djidjeli, K., P.P. Chinchapatnam, P.B. Nair and W.G. Price, 2004. Global and compact meshless schemes for the unsteady convection-diffusion equation. Proceeding of the International Symposium on Health Care and Biomedical Research Interaction, October 08-09, 2004, University of Southampton, Oujda, Morroco, pp: 2-8.

Driscoll, T.A. and A.R. Heryudono, 2007. Adaptive residual subsampling methods for radial basis function interpolation and collocation problems. Comput. Math. Appl., 53: 927-939.

Fasshauer, G.E., 2007. Meshfree Approximation Methods with Matlab. World Scientific Publishers, Singapore,.

Gomez, M.J.A., G.P. Casanova and R.G. Gomez, 2006. Adaptive node refinement collocation method for partial differential equations. Proceeding of the 2006 7th Mexican International Conference on Computer Science, September 18-22, 2006, IEEE, Mexico, ISBN:0-7695-2666-7, pp: 70-80.

Gu, Y. and G.R. Liu, 2006. Meshless techniques for convection dominated problems. Comput. Mech., 38: 171-182.

Kansa, E.J., 1990b. Multiquadrics a scattered data approximation scheme with applications to computational fluid-dynamics II solutions to parabolic, hyperbolic and elliptic partial differential equations. Comput. Mathe. Appl., 19: 147-161.

Kansa, E.J., 1990a. Multiquadrics: A scattered data approximation scheme with applications to computational fluid-dynamics-I surface approximations and partial derivative estimates. Comput. Math. Appl., 19: 127-145.

Li, J., A.H.D. Cheng and C.S. Chen, 2003. A comparison of efficiency and error convergence of multiquadric collocation method and finite element method. Eng. Anal. Boundary Ele., 27: 251-257.

Libre, N.A., A. Emdadi, E.J. Kansa, M. Shekarchi and M. Rahimian, 2008. A fast adaptive wavelet scheme in RBF collocation for nearly singular potential PDEs. Comput. Model. Eng. Sci., 38: 263-284.

Lin, H. and S.N. Atluri, 2000. Meshless Local Petrov-Galerkin (MLPG) method for convection diffusion problems. Comput. Modell. Eng. Sci., 1: 45-60.

Sarra, S.A. and E.J. Kansa, 2009. Multiquadric radial basis function approximation methods for the numerical solution of partial differential equations. Adv. Comput. Mech., 2: 17-206.

Sladek, V., J. Sladek, S.N. Atluri and V.R. Keer, 2000. Numerical integration of singularities in meshless implementation of local boundary integral equations. Comput. Mech., 25: 394-403.

Zhang, S.H. and W.Q. Wang, 2010. A stencil of the finite-difference method for the 2D convection diffusion equation and its new iterative scheme. Int. J. Comput. Math., 87: 2588-2600.